The probabilistic cell: implementation of a probabilistic inference by the biochemical mechanisms of phototransduction

Audrey Houillon, Pierre Bessière, Jacques Droulez

Noname manuscript No.
(will be inserted by the editor)

The probabilistic cell: implementation of a probabilistic inference by the biochemical mechanisms of phototransduction

Audrey Houillon · Pierre Bessière · Jacques Droulez

Received: date / Accepted: date

Abstract When we perceive the external world, our brain has to deal with the incompleteness and uncertainty associated with sensory inputs, memory and prior knowledge. In theoretical neuroscience probabilistic approaches have received a growing interest recently, as they account for the ability to reason with incomplete knowledge and to efficiently describe perceptive and behavioral tasks.

How can the probability distributions that need to be estimated in these models be represented and processed in the brain, in particular at the single cell level?

We consider the basic function carried out by photoreceptor cells which consists in detecting the presence or absence of light. We give a system-level understanding of the process of phototransduction based on a bayesian formalism: we show that the process of phototransduction is equivalent to a temporal probabilistic inference in a Hidden Markov Model (HMM), for estimating the presence or absence of light. Thus, the biochemical mechanisms of phototransduction underlie the estimation of the current state probability distribution of the presence of light. A classical descriptive model describes the interactions between the different molecular messengers, ions, enzymes and channel proteins occuring within the photoreceptor by a set of nonlinear coupled differential equations. In contrast, the probabilistic HMM model is described by a discrete recurrence equation. It appears that the binary HMM has a general solution in the case of constant input. This allows a detailed analysis of the dynamics of the system. The biochemical system and the HMM behave similarly under steady-state conditions. Consequently a formal equivalence can be found between the biochemical system and the HMM. Numerical simulations further extend the results to the dynamic case and to noisy input. All in all, we have derived a probabilistic model equivalent to a classical descriptive model of photransduction, which has the additional advantage of assigning a function to phototransduction. The example of phototransduction shows how simple biochemical interactions underlie simple probabilistic inferences.

Keywords: Phototransduction, Bayesian inference, cell signaling, computational models, vision

1 Introduction

Any subject, or more generally cognitive system, has to reason and acquire new information about its environment from its sensory input. However, some information about the environment can be inaccessible to the subject. These hidden variables influence the sensory inputs but are not taken into account by the subject's representation of its environment. Thus the subject's model of the world he perceives is incomplete. Still, living organisms survive, decide and act efficiently, in spite of perceiving the world with an incomplete model of their environment. Classical computational models usually assume that the brain computes a single estimate of the variable of interest like luminosity, contrast, motion, etc. This can be a problem, as it is the case with ambiguous percepts which are inconsistent with a single value of the variable.

In contrast, probabilistic models assume that the brain estimates the probability corresponding to each possible value of the variable. By probabilistic models we mean subjective probabilistic models (sometimes imprecisely called Bayesian models), signifying that these models describe the world as understood by an observer with some prior knowledge or prior belief about the world (Jaynes

Audrey Houillon
Laboratoire de Physiologie de la Perception et de l'Action, CNRS/Collège de France, Paris, France E-mail: audrey.houillon@college-de-france.fr

Pierre Bessière
Laboratoire d'Informatique de Grenoble, CNRS/Grenoble Universités, Grenoble, France E-mail: bessiere@imag.fr

Jacques Droulez
Laboratoire de Physiologie de la Perception et de l'Action, CNRS/Collège de France, Paris, France E-mail: jacques.droulez@college-de-france.fr

(2003)). The advantage of probabilistic models is that the subject's lack of knowledge is translated as uncertainty: uncertainty about the environment and uncertainty about the models the subject constructs about the physical world. Briefly, the models account for the ability the brain has to reason with incomplete and uncertain knowledge.Therefore, probabilistic approaches have received a growing interest lately, since they have been shown to efficiently describe perceptive and behavioral tasks, as well as multimodal fusion, motor control and pattern recognition (Knill and Richards (2008); Rao et al (2002); Weiss et al (2002); Gold and Shadlen (2002); Ernst and Banks (2002); Körding and Wolpert (2004); Colas et al (2007); Doya et al (2007); Laurens and Droulez (2007); Yang and Shadlen (2007); Bessière et al (2008)). The Hidden Markov Model studied here is a time-dependent form of such a probabilistic inference.

In this study we consider how abstract mathematical computations that have to be estimated in probabilistic models could be represented and implemented in the brain. Different levels of analysis are possible, but so far the most common approach has been population coding. Neural assemblies represent the probabilities to be estimated and the probability can be represented in terms of neuronal activity patterns (Zemel et al (1998); Gold and Shadlen (2002); Ma et al (2006)). At the cellular level intercellular signals, such as spiketrains, have also been considered (Deneve (2008)) as implementing probability distributions. We examine at a lower level how biochemical signaling mechanisms within a single cell, in our case the photoreceptor, may underlie a basic probabilistic inference.

The first steps of the visual process are characterized by the absorption of light by visual pigments in retinal rod and cone photoreceptors and its conversion into graded electrical signals, a process called phototransduction. Electrical signals are then transmitted to bipolar neurons through glutamatergic synapses. The only information a photoreceptor receives about the physical presence of light is the activation of the photopigment rhodopsin evoked by the arrival of a photon. We make the link between the purely descriptive model of these biochemical mechanisms of phototransduction and a probabilistic subjective model, related to a function of the photoreceptor cell. We consider the presumable function carried out by the photoreceptor which consists in detecting the presence or absence of light. One can imagine a theoretical observer that estimates if light is present or absent, based on this new information and on past experience. Hence the probabilistic reasoning perfectly applies to the formalisation of the role the photoreceptor plays, which is similar to that of a theoretical observer which would calculate the probability of presence of the variables representing the state of the world, i.e. the presence or absence of light.

Following Marr's distinction betwen the three levels of information processing (Marr (1982)), the computational function carried out by a photoreceptor cell is to detect the presence or absence of light. The algorithmic level specifies that this computation has to be executed as a probabilistic inference, and can physically be implemented by biochemical phototransduction mechanisms.

In summary, we show that the process of phototransduction can be made equivalent to a temporal probabilistic inference in a hidden markov model, for estimating the presence of light. All in all, a computational function emerges from the interactions between the different molecular messengers, ions, enzymes and channel proteins involved in phototransduction. From the example of phototransduction, we propose that biochemical mechanisms underlie the cell's function of being a basic unit of probabilistic inference.

2 Biochemical Mechanisms of Phototransduction

Phototransduction is at present one of the best described G-protein signaling pathway. The transfer of light information by photoreceptors is highly optimized and covers a wide intensity spectrum. Photoreceptors are specialized in two populations, rods for night vision and cones for daylight . In the following we will mainly focus on vertebrate rod photoreceptors. Rods can detect a single rhodopsin photoisomerisation (Rieke and Baylor (1998b); Sterling (2004)) and have developped adaptation mechanisms for higher intensities.

We consider the biochemical reactions underlying phototransduction in a rod photoreceptor cell as shown in Fig. 1. A detailed description of those mechanisms can be found in (Nikonov et al (2000); Fain et al (2001); Burns and Baylor (2001); Burns and Lamb (2004); van Hateren (2005); Hamer et al (2005)). Briefly, the activation of visual transduction begins with the photoisomerization of the retinaldehyde pigment encapsuled in the transmembrane G-protein coupled receptor (GPCR) rhodopsin, which induces its transformation into an enzymatically activated state (R^*) that catalyzes the activation of many G proteins transducin. Transducin, in turn, activates phosphodiesterase (PDE) which then catalyses the hydrolysis of the diffusible second messenger cyclic guanosine monophosphate (cGMP), with the rate β(t). The consequent reduction of intracellular cGMP leads to the closure of multiple cGMP-gated ion channels in the plasma membrane, thereby blocking the inward flux of Ca^{2+}. Meanwhile, the Na^{2+}/Ca^{2+}, K^+ exchanger continues to pump out Ca^{2+}, so that the intracellular Ca^{2+} concentration declines during illumination. The light-sensitive current is carried by Na^+ and Ca^{2+} ions and the reduction of open channels blocks cation entry, triggering hyperpolarization. This amplification cascade causes at least 10^6 cations to fail to enter the outer segment during a single-photon response (reviewed by Pugh and Lamb (1993)). Just as amplification is essential for the transduction of single rhodopsin molecules into a macroscopic response, timely deactivation is important for a reproducible and accurate time resolution. Recovery of the light response requires the restoration of the cGMP concentration and deactivation of rhodopsin. Calcium regulates the whole molecular process through different feedback mechanisms, such as guanylate cyclase (GC) activity. The modulatory complex GC/GCAP (guanylate cyclase-activating-proteins) synthetizes cGMP from guanosine triphosphate (GTP). But GC/GCAP can also bind to Ca^{2+} thereby inducing a conformational change in the macromolecule GC, decreasing its enzymatical activity and therefore the production of cGMP. As a consequence

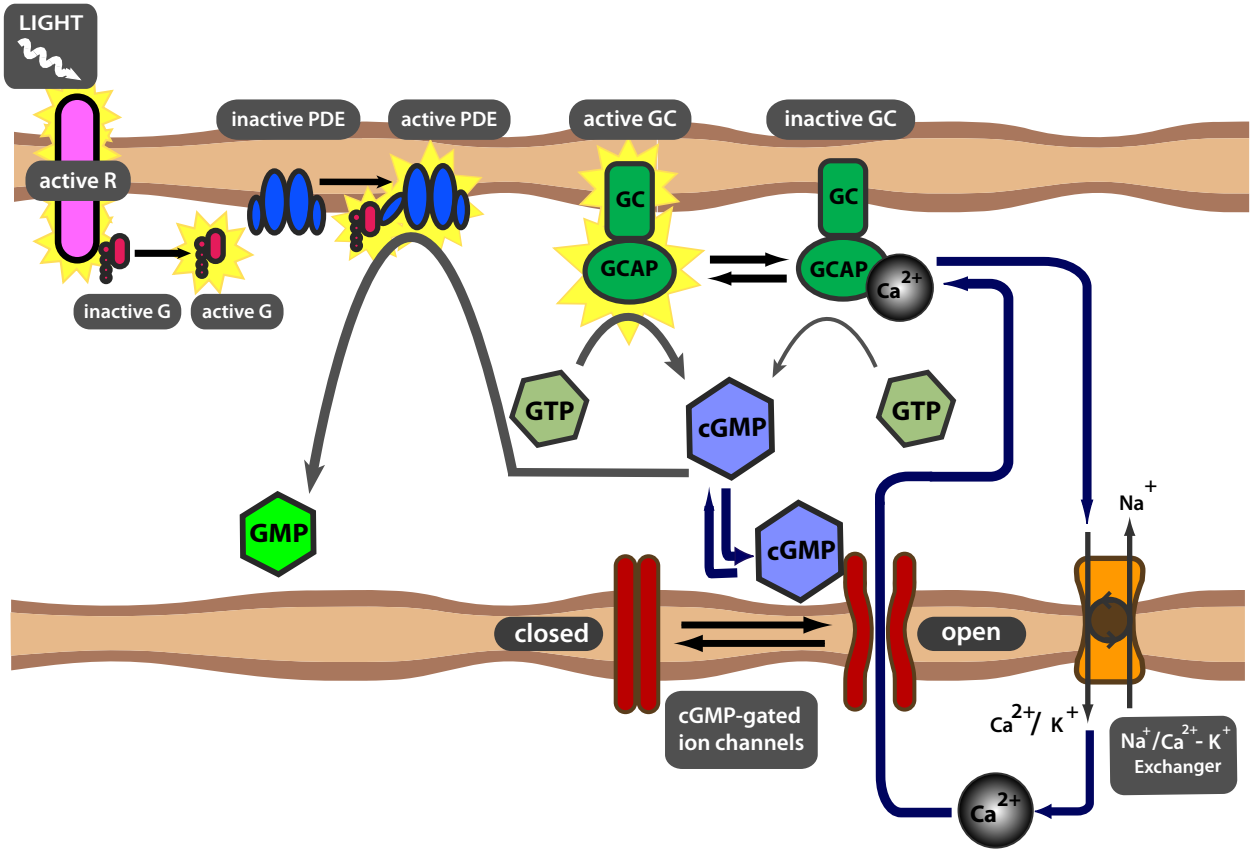

Fig. 1 Simplified description of the biochemical mechanisms of phototransduction: upon absorption of a photon $h\nu$ the photoisomerized rhodopsin molecule R activates the G protein transducin. This amplification front-end reaction in turn activates the phosphodiestarase PDE. PDE catalyses the hydrolysis of cGMP to GMP. The consequent reduction of intracellular cGMP leads to the closure of cGMP-gated ion channels in the plasma membrane, thereby blocking the inward flux of calcium Ca^{2+}.The Na^{2+}/Ca^{2+}-K^{+}exchanger continues to pump out Ca^{2+}, so that the intracellular Ca^{2+} concentration declines during illumination. Calcium in turn regulates GC activity: the complex GC/GCAP catalyzes the production of cGMP out of GTP, but the binding to Ca^{2+}reduces its enzymatical activity and therefore the production of cGMP. Rhodopsin R is turned off by phosphorylations and arrestin binding, whereas transducin and PDE are deactivated by the hydrolysis of GTP (not shown). Various calcium-feedback mechanisms such as the recoverin and calmodulin pathway are not depicted as we do not consider them. Blue arrows represent movements of molecules, black arrows conformational changes and grey arrows enzymatical activity.

GC speeds up the recovery when intracellular calcium decreases. Rhodopsin deactivation depends on multiple steps of rhodopsin phosphorylation (Rieke and Baylor (1998a); Whitlock and Lamb (1999)), which is catalysed by rhodopsin kinase. Arrestin binding follows rhodopsin phosphorylation, quenching its remaining activity. Other calcium-dependent adaptation mechanisms exist, as the inactivation of rhodopsine kinase by calcium-bound recoverin or closing of ionic channels by calcium-bound calmodulin. For our purpose we don't consider calcium modulation of recoverin and calmodulin activities, i.e. the rate constant of rhodpsin decay is taken as constant. This simplification has only limitations in the case of incremental flash responses with background adaptation. In this case the amplitude of the response is slightly smaller than expected from more complex theoretical models (Nikonov et al (2000); Hamer et al (2005)). Turning-off transducin and PDE is also essential for a timely and reproducible deactivation of the light-response. The hydrolysis of GTP to GDP (accelerated by the RGS9-1 protein) causes transducin to dissociate from the gamma subunit of PDE, allowing gamma to reinhibit PDE's catalytic activity, thereby deactivating both proteins. The rate-limiting step of light-recovery is certainly the deactivation of rhodopsin (Rieke and Baylor (1998a)) or transducin/PDE (Sagoo and Lagnado (1997)). In order to generate useful signals across a light intensity range of several orders of magnitude light adaptation reduces the cell's sensitivity. In rods, the steady-state response amplitude to light intensity is highly nonlinear and saturates for high values (Hodgkin and Nunn (1988); Koutalos et al (1995)). Furthermore, background light reduces the amplitude of incremental flash response over a considerable range and the sensitivity to an incremental flash of same intensity varies inversely to steady background intensity, a relation known as Weber's law (Burkhardt (1994); Perlman and Normann (1998); Pugh et al (1999)). This background adaptation is effected by calcium-dependent mechanisms (regulation of PDE activity via recoverin, regulation of GC via GCAP's, regulation of cGMP-gated channels via calmodulin).

The present simplified descriptive model of phototransduction delineates the chemical and differential equations used in the simulations and is adapted mainly from the work done in (Nikonov et al (2000); Hamer et al (2005)). The concentrations are considered as homogeneous across the cell compartment.

Light input $I(t)$ triggers rhodopsin activity. Activated rhodopsin R^* is deactivated by rhodopsine kinase (RK). Recoverin feedback on rhodopsine kinase was neglected here

$$\frac{\mathrm{dR}^*}{\mathrm{dt}} = I(t) - k_R R^* \tag{1}$$

Activated rhodopsin R^*, via transducin, induces an increase in the number of active PDE molecules PDE^*. The number of active PDE^* molecules is depleted with a rate proportional to its number

$$\frac{\mathrm{dPDE}^*}{\mathrm{dt}} = \nu_{R-PDE} R^* - k_{PDE} PDE^* \tag{2}$$

The total reaction rate constant of cGMP hydrolysis $\beta(t)$ is

$$\beta(t) = \beta_{\mathrm{dark}} + \beta_{\mathrm{sub}} PDE^* \tag{3}$$

with β_{dark} the dark spontaneous cGMP hydrolysis rate constant and β_{sub} the rate constant of cGMP hydrolysis per activated PDE* unit . The hydrolysis ofcGMP by PDE^* decreases the cGMP concentration $[cGMP]$ with rate constant β(t). In contrast, the guanylate cyclase GC raises the cGMP concentration $[cGMP]$ with activity α(t)

$$\frac{d[cGMP]}{dt} = \alpha(t) - \beta(t)[cGMP] \tag{4}$$

Ca^{2+} regulation of GC activity is mediated by GCAP's and biochemical studies (Dizhoor and Hurley (1999)) have shown that at low calcium levels GCAP activate GC's, whereas at high calcium concentrations the calcium-bound forms of GCAP's inhibit GC activity (reviewed in Pugh et al (1997)). Calcium reversibly associates with the membrane macromolecule complex GC/GCAP. This macromolecule has a specific receptive site for the ligand Ca^{2+} and the calcium-bound form induces a conformational change in the macromolecule. Calcium activation seems to be cooperative, with reported Hill coefficient n_{cyc} between 1 (van Hateren (2005)) and 4 (Koch and Stryer (1988)), and values for half-maximal activity concentration $\mathrm{K_{cyc}}$ vary widely depending on experimental conditions. The common empirical form of the Hill equation for GC reaction rate α(t) was used (Koch and Stryer (1988); Pugh et al (1997)), with n_{cyc}=1 , fitted to the GC activity described in Nikonov et al (2000)

$$\alpha(t) = \rho + \frac{\gamma}{1 + \frac{[Ca^{2+}]}{K_{cyc}}} \tag{5}$$

cGMP binding opens cGMP-gated ion channels, thus indirectly controlling the inflow of Ca^{2+} via ionic channels, with a factor η. On the other direction the Ca^{2+} concentration $[Ca^{2+}]$ is reduced by the $\mathrm{Na^{2+}/Ca^{2+}}$, $\mathrm{K^+}$ -exchanger by a factor κ:

$$\frac{d[Ca^{2+}]}{dt} = \eta[cGMP] - \kappa[Ca^{2+}] \tag{6}$$

Altogether the equations (1) to (6) form a system of nonlinear coupled differential equations. The definitions and values of the parameters of the phototransduction model are listed in Table 1 and are taken from vertebrate, mostly amphibian rods. With this model we can describe light and dark adaptation over a wide range of intensities, as well as dim flash responses, as shown when comparing with experimental data on vertebrate photoreceptors and results by Nikonov et al (2000). The model works well despite the fact that we simplified some interactions and did not include all feedback pathways, such as the recoverin, calmodulin and arrestin pathways.

3 Probabilistic inference: the Hidden Markov Model (HMM)

In this section we introduce the simplest form of time-dependent probabilistic inference, namely the Hidden Markov Model (HMM) (see comprehensive review in Rabiner (1989)). The HMM is widely used in probabilistic modeling as the base for more complex models. A random variable S^t describes the state of the world at time t, as seen from the viewpoint of the observer. Probability distributions over this space state are used to describe the subject's current knowledge. The current knowledge is then continuously updated with new observations about the world, which are delivered by the sensory receptors. An observation made at time t is termed O^t. The HMM observer model is called "hidden" markov model, because the observer has never access to the actual value of the state S^t. Only observations of the state (which may be uncertain) are directly available. The updated knowledge, called posterior probability distribution $P(S^{0:t}|O^{0:t})$, can then be used by the observer to choose an appropriate action. The label $0:t$ means that the observer takes into account all the observations $O^{0:t}$ made from time 0 to t, and $S^{0:t}$ are the values of all the corresponding world state S^t from time 0 to t.

Parameter	Value	Definition	Reference
κ	$39.35\,s^{-1}$	Rate constant of Ca^{2+} extrusion by the Na^{+}/Ca^{2+}-K^{+} exchanger	derived from data in Hamer et al. 2005
η	$9.13\,s^{-1}$	Rate constant of Ca^{2+} influx through cGMP-gated cation channels	derived from data in Hamer et al. 2005
K_{cyc}	$0.06\,\mu M$	Ca^{2+} concentration for half-maximal cyclase activity (for n_{cyc} =1)	derived from data in Nikonov et al. 2000
γ	$50\,\mu M \cdot s^{-1}$	Maximal value of α at low Ca^{2+} concentration	derived from data in Nikonov et al. 2000
ρ	$0.01\,\mu M \cdot s^{-1}$	Minimal value of α at very high Ca^{2+} concentration	derived from data in Nikonov et al. 2000
k_{on}	$2500\,s^{-1}$	Rate constant of spontaneous PDE* activation	derived from data in Hamer et al. 2005
k_{off}	$0.45\,s^{-1}$	Rate constant of inactivation of spontaneously activated PDE*	Hamer et al. 2005
ν_{RPDE}	$220\,s^{-1}$	Rate of activated PDE* formation per fully activated R*	Nikonov et al. 2000
k_{Rmax}	$12\,s^{-1}$	Rate constant of R* inactivation when all RK is free	Nikonov et al. 2000
k_{PDE}	$0.625\,s^{-1}$	Rate constant of inactivation of the G*-PDE* complex	Nikonov et al. 2000
β_{dark}	$1\,s^{-1}$	Rate constant of cGMP hydrolysis in dark	Nikonov et al. 2000
β_{sub}	$1.8 \cdot 10^{-4}\,s^{-1}$	Rate constant of cGMP hydrolysis per activated PDE* subunit	Nikonov et al. 2000
Ca_{dark}	$0.806\,\mu M$	Cytoplasmic concentration of Ca^{2+} in dark	calculated
$cGMP_{dark}$	$3.474\,\mu M$	Cytoplasmic concentration of cGMP in dark	calculated
PDE_{dark}	$10\,nM$	Cytoplasmic concentration of activated PDE* in dark	calculated, Rieke & Baylor 1996
R_{dark}	$0\,\mu M$	Cytoplasmic concentration of activated R* in dark	Nikonov et al. 2000

Table 1 Parameters of the phototransduction model

We consider the photoreceptor cell as operating in a fashion that ressembles that of an observer. Based on prior knowledge, given by past experience (i.e. $P(S^{0:t-\Delta t}|O^{0:t-\Delta t})$) and present observations O^t, the theoretical photoreceptor observer estimates the probability of the presence or absence of light $P(S^{0:t}|O^{0:t})$ at time t. The presence or absence of light at time t is defined as the binary state S^t (one for the presence of light $S^t = 1$ and one for the absence of light $S^t = 0$). We assume a constant time interval Δt between two observations O^t and $O^{t+\Delta t}$. Δt is chosen to be in concordance with natural integration times of phototransduction, i.e. in the ms range or less. The photoreceptor is a photon detector that integrates the arrival of single photons over time (Rieke and Baylor (1998b)). The aim of the theoretical observer is to estimate the posterior probability distribution $P(S^{0:t}|O^{0:t})$. Some simplifications can be made regarding the conditional dependencies to only one time step Δt back and with the following three assumptions for an HMM:

1. Markov property of order 1, that is the conditional probability distribution of the present state depends only upon the preceding state : $P(S^t|S^{0:t-\Delta t}) = P(S^t|S^{t-\Delta t})$
2. The distribution on the present state S^t is independent on anything else before, given the preceding state: $P(S^t|S^{0:t-\Delta t}O^{0:t-\Delta t}) = P(S^t|S^{t-\Delta t})$ refered to as the photoreceptor's world-model.
3. Past observations and states do not have direct incidence on the sensory receptor, so that the distribution on the present observation is independent on anything else before, given the present state: $P(O^t|S^{0:t}O^{0:t-\Delta t}) = P(O^t|S^t)$, refered to as the photoreceptor's sensor-model.

Taken together, the world- and sensor models and the initial prior $P(S^0)$ define the decomposition of the joint probability distribution $P(S^{0:t}O^{0:t})$, simplified to

$$P(S^{0:T}O^{0:T}) = P(S^0)\prod_t^T P(S^t|S^{t-\Delta t})P(O^t|S^t) \tag{7}$$

The bayesian inference is done in two steps. First, the prediction step is done by using the past and present knowledge, then comes the updating step by including the new observation to actualise the prediction.

– Prediction step: from the previous probability distribution, that is the last estimation over S^t given all past and present observations made by the photoreceptor, we obtain the prediction, ie. the probability distribution over $S^{t+\Delta t}$ by a marginalization process over the present state S^t. The transition probabilities $P(S^{t+\Delta t}|S^t)$ correspond to the observer's expectations about the changing of states.

$$P(S^{t+\Delta t}|o^{0:t}) = \sum_{S_t} P(S^t|o^{0:t})P(S^{t+\Delta t}|S^t) \tag{8}$$

– Updating step: the prediction step gives the prior knowledge for the next time step. This "prior knowledge" is then refreshed by an inference with the new observation $o^{t+\Delta t}$ to compute the new posterior probability distribution

$$P(S^{t+\Delta t}|o^{0:t+\Delta t}) \propto P(S^{t+\Delta t}|o^{0:t})P(o^{t+\Delta t}|S^{t+\Delta t}) \tag{9}$$

We suppose that the transition matrix is time invariant, ie. the transition probabilities are independent from the point in time: $P(S^{t+\Delta t} = 1|S^t = 0) = T_{01}$ and $P(S^{t+\Delta t} = 0|S^t = 1) = T_{10}$, with the constants T_{01} and T_{10}. The transition probabilities T_{01} and T_{10} describe how likely the state S^t is expected to change, from the viewpoint of the observer. Small values of T_{01} and T_{10} mean that the

observer expects the world to be stable, high values on the contrary mean that the state is expected to rapidly change. For a binary state, the posterior distribution is completely defined by the ratio

$$u(t) = \frac{P(S^t = 1|o^{0:t})}{P(S^t = 0|o^{0:t})} \tag{10}$$

of the two possible posterior probabilities (one for the presence of light, i.e $S^t = 1$ and one for the absence of light, i.e. $S^t = 0$). A high value of $u(t)$ means that the presence of light is more probable than the absence of light, given all the observations that have been made so far. The updating rule can thus be reduced to the form

$$u(t+\Delta t) = f(t+\Delta t)\frac{T_{01} + (1-T_{10})u(t)}{1 - T_{01} + T_{10}u(t)} \tag{11}$$

where we define the likelihood ratio

$$f(t+\Delta t) := \frac{P(o^{t+\Delta t}|S^{t+\Delta t} = 1)}{P(o^{t+\Delta t}|S^{t+\Delta t} = 0)} \tag{12}$$

and the prediction ratio $v(t+\Delta t) := \frac{T_{01}+(1-T_{10})u(t)}{1-T_{01}+T_{10}u(t)}$. The likelihood ratio $f(t)$ provides an insight on the likeliness of having a specific observation given that light was present versus having that same observation given that light was absent. A high value of $f(t)$ for example means that the observation is more likely to be made when light was present.

In this way the current state probability distributions, represented by $u(t)$, are continously updated by the flow of obervations, represented by $f(t)$. The issue is now to exhibit how these abstract mathematical algorithms can be carried out by the molecular interactions underlying phototransduction and how the biochemical parameters and variables are related to the probabilistic parameters and probability distributions, as will be shown in section 4. We first consider the particular case of the stationary HMM to get a general view of the characteristics of the HMM.

3.1 Solution of the stationary HMM

The analysis of the dynamics of the stationary binary HMM, i.e. with constant input $f(t) = f$, yet provides us with a good insight in the general dynamics of the HMM. The likelihood ratio $f(t) = f$ is called the "input" to the HMM, as it reflects the observations of the presence or absence of light in the probabilistic framework. In this section, we demonstrate that the stationary binary HMM has an explicit solution, which converges to a steady value u. For a constant input, i.e. constant likelihood ratio

$$f = \frac{u(1 - T_{01} + T_{10}u)}{T_{01} + (1 - T_{10}u)} \tag{13}$$

the recurrent discrete-time HMM equation (11) can be solved analytically. The equation has the form

$$u_{n+1} = \frac{a + ru_n}{1 + \frac{u_n}{m}} \tag{14}$$

if we write

$$a = \frac{fT_{01}}{1 - T_{01}}, \qquad r = \frac{f(1-T_{10})}{1 - T_{01}}, \qquad m = \frac{(1-T_{01})}{T_{10}}, \qquad \text{with a, m and r} \quad > 0 \tag{15}$$

This equation closely resembles a Beverton-Holt equation (BH) , the only difference being the additional constant term a.

$$y_{n+1} = \frac{Ru_n}{1 + \frac{u_n}{M}} \tag{16}$$

The Beverton-Holt equation is known to have a closed form solution (with initial condition y_0 and time step $n \in \mathbb{N}$)

$$y_n = \frac{(R-1)M}{1 + (\frac{(R-1)M - y_0}{y_0})R^{-n}} \tag{17}$$

We can transform eq. (14) to a classical BH eq. (16) by appling the variable substitution $x_n = u_n - u$ and we consequently find a closed-form solution of eq. (14). u corresponds to the steady-state solution of the HMM equation (14) for $u_{n+1} = u_n$.

The exact solution of this equation writes

$$x_n = \frac{(r-1)m - 2u}{1 + \left(\frac{(r-1)m - 2u - x_0}{x_0}\right)\left(\frac{(rm-u)}{(m+u)}\right)^{-n}} \tag{18}$$

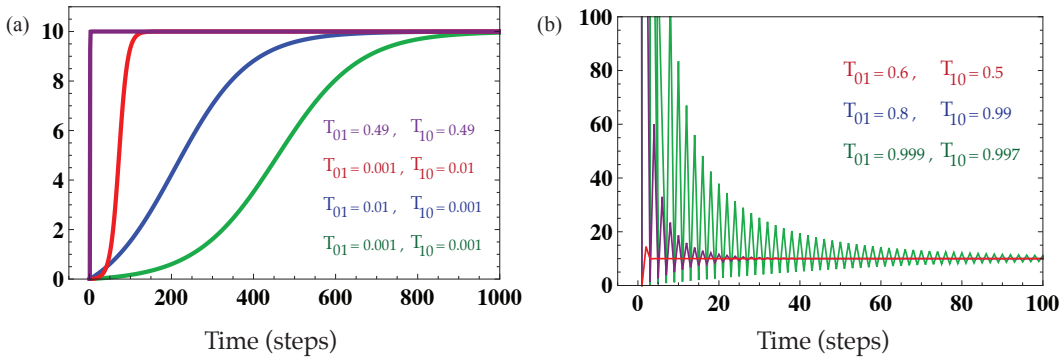

Fig. 2 Dynamics of the HMM with constant input. (a) Subcritical case for various combinations of T_{01} and T_{10} (indicated by color index). The more $T_{01}+T_{10}$ differs from 1 the slower is the convergence (b) Supercritical case for various combinations of T_{01} and T_{10} (indicated by color index). The more $T_{01}+T_{10}$ differs from 1, the slower the convergence and the damped oscillations around u more intense.

The solution of the HMM for a constant input f can be deduced by replacing the parameters a, r and m with their equivalent functions of u, T_{01} and T_{10} from eq. (15)

$$u_n = u + \frac{u^2(T_{10}-1)T_{10} - 2uT_{01}T_{10} + T_{01}(T_{01}-1)}{T_{10}(T_{01}+u-T_{10}u)\left(1 + \frac{(T_{01}(1-T_{01}+T_{10}u)T_{10}(T_{01}+u-T_{10}u))\left(\frac{(T_{01}+T_{10}-1)u}{(T_{01}-T_{10}u-1)(T_{01}+u-T_{10}u)}\right)^{-n}}{(u-u_0)(T_{10}(T_{01}+u-T_{10}u))}\right)} \tag{19}$$

The behavior of the solution (19) mainly depends on the sign of the term in the power of $-n$: if the term is negative it will change its sign at each step and thereby the solution u_n will converge with damped oscillations to the steady-state value u. On the opposite, when the term is positive it will always keep the same sign and u_n will converge in a monotous way to u.

The denominator is always negative, independently of the value of T_{01} and T_{10}. The nominator is negative for $T_{01}+T_{10}<1$, whereas it is positive for $T_{01}+T_{10}>1$. Thus we can distinguish three cases, dependent on the values of T_{01} and T_{10}:

- **Critical condition** ($T_{01}+T_{10}=1$)**:** The whole second term in equation (19) vanishes, so that the solution is equal to u at the first step.
- **Subcritical condition** ($T_{01}+T_{10}<1$) : The term in the power of n is positive, therefore we have a monotonous convergence towards u. The more $T_{01}+T_{10}$ differs from 1 the slower is the convergence. Some example are shown in Fig. (2 a) for u=10 and u_0=0.
- **Supercritical condition** ($T_{01}+T_{10}>1$) **:** The term in the power of n is negative, therefore we have a convergence towards u with damped oscillations. As in the subcritical case, the more $T_{01}+T_{10}$ differs from 1, the slower is the convergence. Some examples are shown in Fig. (2b)

The convergence to u can be proven in all three cases. For $n\to\infty$, we have $u_n\to u$, which agrees with the steady-state solution u of eq. (14). Another interesting point is that the steady-state value u doesn't depend on the initial condition u_0, that is u_0 is only present in the second –to zero converging– term of solution (19). In fact u only depends on the transition probabilities T_{01}, T_{10} and the input f.

4 Steady-state equivalence

The two models described so far have different intrinsic characteristics. The probabilistic filter has a discrete time representation with two computational steps and can be defined by two variables, the posterior probability ratio $u(t)$ and the likelihood ratio $f(t)$, whereas the biochemical processes are characterised by differential equations in three variables: the concentrations of $[cGMP]$ and $[Ca^{2+}]$ and $\beta(t)$, the rate constant of cGMP hydrolysis. In addition the phototransduction model has more parameters. Nevertheless, the rationale of our approach is to analyse the constraints under which the HMM and the biochemical system converge to the same solution. We have to find a way to relate the "outputs" of both systems to each other, i.e. the calcium concentration $[Ca^{2+}]$ and the posterior pobability ratio $u(t)$. In a similar way the "inputs" of both systems, the likelihood ratio $f(t)$ and the rate constant of cGMP hydrolysis $\beta(t)$, must also be linked together. To this end we derive, under steady-state conditions, a formal equivalence between the probabilistic inference and the biochemical mechanisms. Hence, we require the input to both systems to be constant: $\beta(t)=\beta$ in the biochemical system and $f(t)=f$ in the HMM. Notice that we define the "input" as being $\beta(t)$, the preprocessed function of the light intensity $I(t)$ and not the light intensity itself. $\beta(t)$ is an amplified form of $I(t)$, with slower dynamics due to a relatively long time constant k_{PDE}.

At steady-state the HMM updating ratio rule is a quadratic equation

$$u^2 + u\left(\frac{1-T_{01}}{T_{10}} - \frac{f(1-T_{10})}{T_{10}}\right) - f\frac{T_{01}}{T_{10}} = 0 \tag{20}$$

For the biochemical model, the (chemical) steady-state condition implies that the biochemical variables $[Ca^{2+}]$ and $[cGMP]$ are constant. Those assumptions also yield a quadratic equation in $[Ca^{2+}]_{ss}$, the steady calcium value:

$$[Ca^{2+}]_{ss}^2 + [Ca^{2+}]_{ss}\left(K_{cyc} - \frac{\eta\rho}{\beta\kappa}\right) - \frac{\eta K_{cyc}(\rho+\gamma)}{\kappa\beta} = 0 \tag{21}$$

Our fundamental assumption is that the calcium concentration $[Ca^{2+}]$ encodes the posterior probability distribution ratio $u(t)$. The link between the probabilistic filter and its biochemical implementation is then given by setting the proportionality

$$[Ca^{2+}]_{ss} = \lambda \cdot u \tag{22}$$

with constant λ (μM). Replacing $[Ca^{2+}]_{ss}$ in eq. (21) and comparing with eq. (20) yields the relations between the parameters of the probabilistic model and the biochemical system. We get a first relation, with the constraint that f has to be solely dependent on the biochemical input β, but not on T_{01} and T_{10}.

$$T_{01}(\lambda) = \frac{(\gamma+\rho)(\lambda - K_{cyc})}{\lambda\gamma}, \qquad T_{10}(\lambda) = \frac{K_{cyc}(\gamma+\rho) - \lambda\rho}{\gamma K_{cyc}}, \qquad f(\lambda,\beta) = \frac{\eta\,(K_{cyc}(\gamma+\rho) - \lambda\rho)}{\beta\kappa\lambda\,(\lambda - K_{cyc})} \tag{23}$$

Note that the biochemical system and the HMM may not have the same evolution during transient regimes but they will converge to the same stable steady-state solution, if we use parameters satisfying eq. (23). In fact, the stability of the biochemical steady-state solutions can also can be demonstrated (not shown).

For relation (23) and the biochemical parameters of phototransduction listed in Table 1, the values of the transition probabilities are constrained to the fixed values $T_{01} = 0.940$ and T_{10}= 0.996. These values are close to 1, which means that the state is expected to change with a very high probability on the next step. In other words the observer expects the world to be highly unstable and doesn't rely a lot on the past history to predict the next step. Instead, the prediction oscillates around the real value towards steady state in the supercritical case (which involves high values of transition probabilities), as shown in Fig. 2 for a steady input. To prevent overshooting, the predictions have to be "corrected" by the observations.

A more general relation allowing an arbitrary choice of T_{01} and T_{10} can be derived from u, the steady state value of the posterior ratio $u(t)$:

$$u = \frac{[Ca^{2+}]_{ss}}{\lambda} = \frac{\eta\rho - \beta K_{cyc}\kappa + \sqrt{(\beta\kappa K_{cyc})^2 + (\eta\rho)^2 + 2\beta K_{cyc}\eta\kappa(2\gamma+\rho)}}{2\lambda\beta\kappa} \tag{24}$$

In order for the HMM to converge to the same steady-state value λu the condition on f, for an arbitrary choice of T_{01} and T_{10}, is given by the inverse relation of eq. (20)

$$f(\beta, T_{01}, T_{10}) = u \cdot \frac{1 - T_{01} + T_{10}u}{T_{01} + (1 - T_{10})u} \tag{25}$$

Altogether, with relations (24) and (25), the transition probabilities can thus be choosen accordingly to be in the subcritical case, i.e. without oscillations around the steady-state.

5 Extension to Dynamical Case

We want to verify if the equivalence between the HMM and its biochemical implementation, i.e. $[Ca^{2+}] = \lambda u(t)$, still holds for the dynamical case, that is for time varying light intensities, as photoreceptors as usually exposed to in normal environments. As neither system has a (known) general analytical solution, we propose to compare the solutions found in numerical simulations for different natural time-varying inputs $\beta(t)$, depending on the light intensity $I(t)$, and its corresponding $f(t)$, as defined at steady-state (here for $\lambda = 1$ and Δt = 1ms).

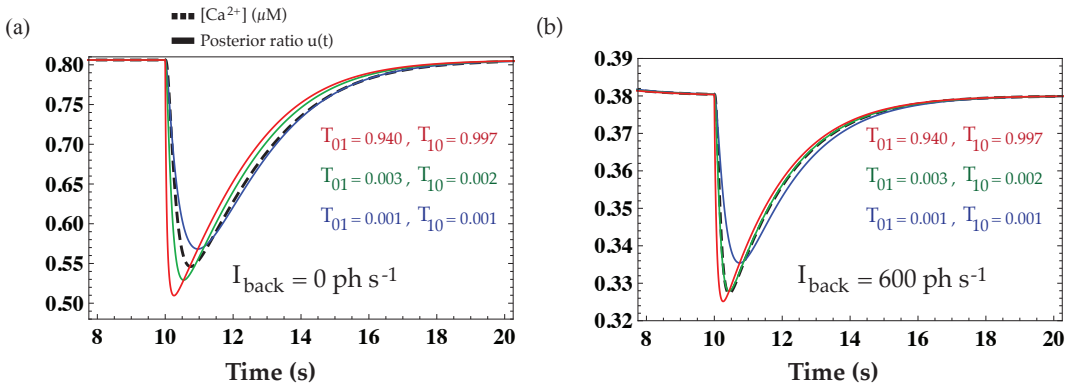

Fig. 3 Comparison of calcium and $u(t)$ for different combinations of T_{01} and T_{10} (given by color index) (a) dark-adapted flash of duration 10 ms and intensity 2000 photoisomerisation per flash presented and at t=10 s (b) same flash as in (a) superimposed on a steady background of light intensity $I(t) = I_{back}$(1-exp(-100t)), presented at t=10 s. I_{back}=600 photoisomerisation s^{-1}. Dotted black line represents the calcium concentration, full line represent corresponding posterior ratio u(t). Combinations of $T_{01} + T_{10}$ close to 1 have more rapid dynamics and can become faster then the calcium response.

5.1 Deterministic input

The time evolution of $[Ca^{2+}]$ and $u(t)$ was compared in Fig. 3 for different combinations of T_{01} and T_{10} for a dark-adapted flash of duration 10 ms (a) and a flash superimposed on a steady background light of intensity I_{back} (b). As expected from the steady-state behavior, the HMM response has a different delay compared to the calcium response, depending on the transition probabilities. Nonetheless, the posterior ratio solutions are very close to $[Ca^{2+}]$. For the natural light intensities tested ranging from 0 to 8000000 ph s^{-1}, very low intensity oscillations are present during the initial 0.01s of the response in the supercritical case, but cannot be seen on the scale of the graphs because they are so small. More generally the amplitude of $u(t)$ and the delay to the calcium response depend on the value of $T_{01} + T_{10}$, values close to 1 appearing to have faster dynamics (as in steady-state). But the relation is more complex and also depends on the temporal and intrinsic characteristics of the input itself in a nontrivial way. Besides, the compression of the flash response for increasing background light is in accordance with the results in Nikonov et al (2000).

Fig. 4 shows $[Ca^{2+}]$ and $u(t)$ responses for the subcritical values $T_{01} = T_{10} = 0.1$. The results for different types of time-varying light intensities were simulated for an illumination converging to a steady state (a), for a periodic lighting (b) for a flash of 10 ms duration in dark-adapted condition (c) and for the same flash superimposed on a steady background intensity I_{back}=600 photoisomerisation s^{-1} (d), respectively for three distinct peak amplitudes. In all conditions the posterior ratio $u(t)$ and the calcium concentration have very similar trajectories. Altough the probabilistic inference has a slightly faster response for these specific values of T_{01} and T_{10}, as predicted both responses converge to the same steady state value. The flash responses of different intensities in (c) and (d) show the hallmark of light adaptation, consistent with the studies in Nikonov et al (2000): reduction of flash sensitivity with increasing background light, decrease in time to peak and longer recovery time for increasing flash intensity.

5.2 Stochastically fluctuating input

The limit on photon counting accuracy is imposed by dark noise in rod photoreceptors. Two main components of dark noise can be recorded in the single photon response (citetbayloretal1980): discrete events arising from the spontaneous activation of rhodopsin and a continuously present fluctuation arising from the spontaneous activation of individual catalytic subunits of PDE (Rieke and Baylor (1996)). In addition to internal dark noise, the quantal nature of light, i.e. Poisson fluctuations in the number of absorbed photons, is another source of stochastic fluctuation. The internal and external noise sources are independent and additive, and can be described by Poisson statistics (Rieke and Baylor (1998b); Chichilnisky and Rieke (2005)). To take the stochastic nature of the photon arrival into account, as well as spontaneous rhodopsin and PDE activity, we included their contribution in stochastic fluctuations of the input. For our purpose we need a noisy input that phenomenologically ressembles a realistic noise found in rods, without requiring to simulate in details each possible source of fluctuations in the biochemical pathway from rhodopsin to PDE. Therefore we used a hybrid stochastic/deterministic model, i.e. we only sample stochastically the dominant molecular interactions responsible for the noise described before, and injected the resulting fluctuating PDE activity $\beta(t)$ as the input to the differential equations describing the remaining biochemical pathway or the corresponding probabilistic inference. The results are shown in Fig 5 for an illumination converging to a steady state (a) and for a flash in dark-adapted condition (b). As for the deterministic input the posterior ratio $u(t)$ and the calcium concentration have similar trajectories and the probabilistic inference still has a slightly faster response for the values $T_{01} = T_{10} = 0.1$. Both responses fluctuate, which is especially visible around the steady state. $[Ca^{2+}]$ fluctuates less, probably because of the intrinsic characteristic of the biochemical system which tends to smooth out the noise. For very small values of T_{01} and T_{10} the

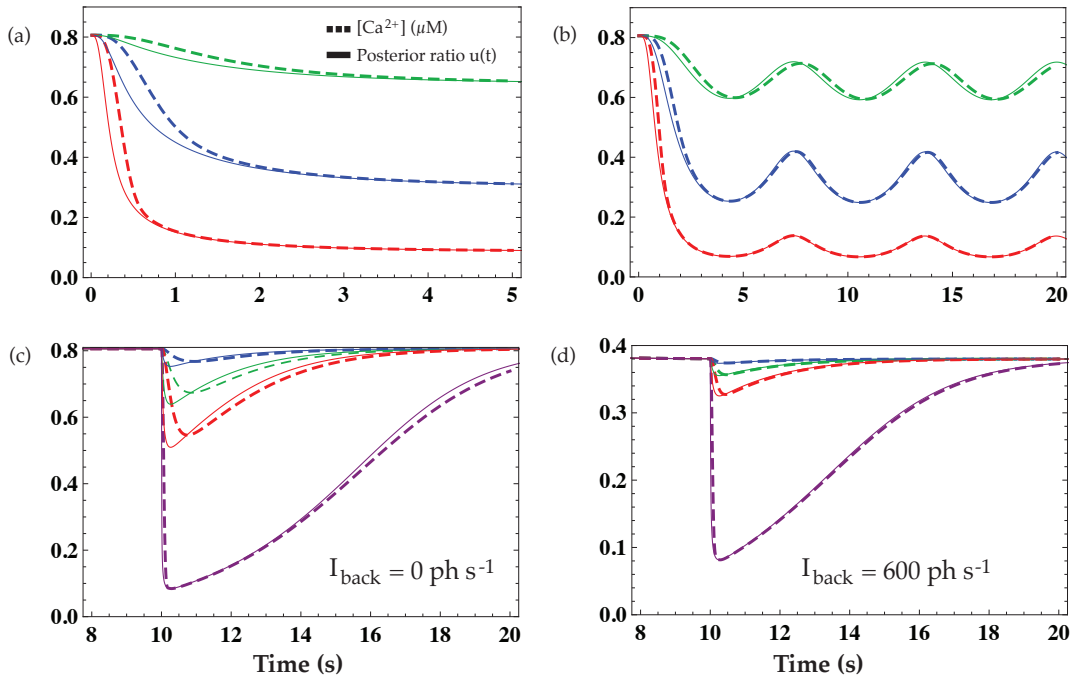

Fig. 4 Comparison of calcium and posterior ratio for subcritical case with $T_{01} = T_{10}$= 0.1 and different light intensities $I(t)$. (a) Illumination converging to a steady state $I(t) = I_0$(1-exp(-100t) for I_0=100, 1000 and 10000 ph s^{-1} (b) Periodic illumination I_0(1-cos(t)) for I_0=100, 1000 and 10000 ph s^{-1} (c) Flash of 10 ms duration in dark-adapted condition for flash intensities 200, 800, 2000 and 85000 ph per flash (d) Flash superimposed on a steady background intensity I_{back}=600 ph s^{-1}. Flash intensities as in (c). In all conditions the posterior ratio $u(t)$ and the calcium concentration have very similar trajectories, however the probabilistic inference has a slightly faster response.

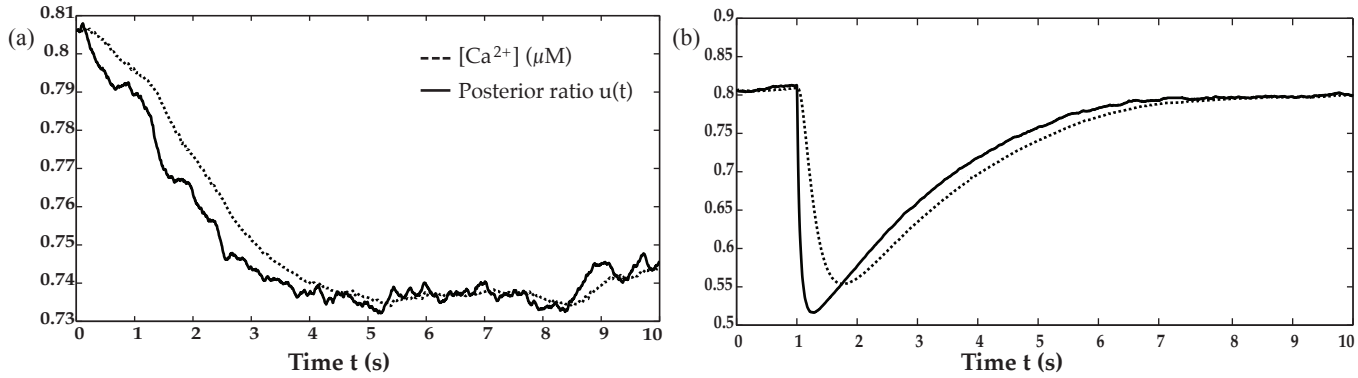

Fig. 5 Comparison of calcium and posterior ratio for subcritical case with $T_{01} = T_{10}$= 0.1 and stochastically fluctuating input. (a) Illumination converging to a steady state $I(t) = I_0$(1-exp(-100t) for I_0=30 ph s^{-1} (b) Flash of 10 ms and intensity 2000 photoisomerisations per flash, presented at t=1 s in dark-adapted condition.

HMM response is less sensitive to fluctuations (not shown here), due to the low probability of changing state in the prediction step, but in turn the response kinetics are slower.

6 Discussion

The specific function of photoreceptors is to detect and transform light stimuli in electrical signals, a process called phototransduction. We have considered the biochemical reactions underlying phototransduction and have described the complex biochemical interactions by a set of coupled differential equations. Noise originating from the stochastic nature of the photon arrival time, as well as spontaneous rhodopsin and PDE activity were also taken into account. Additionally, we have shown that the photoreceptor cell behaves like a temporal probabilistic inference filter in a Hidden Markov Model. To infer the state of the world (i.e the presence or absence of light), the process of phototransduction underlies the estimation of the current state probability distribution ratio $u(t)$.

This computational function emerges from the interaction between the different molecular components of phototransduction. Our probabilistic filter model is equivalent to a classical descriptive model of rod phototransduction but is described by much simpler equations. From this knowledge it would be possible to derive the functional circuits involved in the processing of visual information and to mimic the photoreceptor coding of information. The link between the descriptive and the probabilistic functional model was derived under steady-state conditions. It was then extended to the dynamical case. It appeared that the HMM displayed two types of dynamics, depending on the combination of transition probabilities T_{01} and T_{10}. However, the detailed response further depends on the temporal and intrinsic characteristics of the input and as a result $u(t)$ slightly differs from $[Ca^{2+}]$. The calcium response rapidly adapts to the input, a feature the HMM model lacks. Our model could be extended by including more calcium-dependent feedback loops such as the signaling pathways of recoverin, calmodulin and arrestin, to better reproduce calcium dynamics. While including additional state variables would possibly yield more realistic phototransduction and subjective probabilistic models, our results yet show that relatively simple biochemical interactions can represent probabilistic inferences. Not only that our probabilistic model provides a systems-level analysis of phototransduction but it also provides a foundation for understanding the generic principles of G protein signaling. Our probabilistic inference model could be extended to primary sensory transduction in general given the similarity with other sensory transduction systems. Indeed, it has be pointed out that there are common strategies of transduction in different sensory sytems (Shepherd (1991); Torre et al (1995); Frings (2009)). Altough the detailed biochemical implementation level would to have be adapted, the principles described here could be applied to other sensory cells and neurons in general, as the computational and algorithmic principles would still hold .

Aknowledgments

This work was supported by European program BACS (Bayesian Approach to Cognitive Systems) FP&-IST-027140. We also thank Francis Colas for fruitful discussions and Michael Zugaro for giving helpful comments on the manuscript.

References

Bessière P, Laugier C, Siegwart R (eds) (2008) Probabilistic Reasoning and Decision Making in Sensory-motor Systems (Springer Tracts in Advanced Robotics). Springer

Burkhardt DA (1994) Light adaptation and photopigment bleaching in cone photoreceptors in situ in the retina of the turtle. The Journal of neuroscience : the official journal of the Society for Neuroscience 14(3 Pt 1):1091–1105

Burns ME, Baylor DA (2001) Activation, deactivation, and adaptation in vertebrate photoreceptor cells. Annual review of neuroscience 24:779–805

Burns ME, Lamb TD (2004) Visual transduction by rod and cone photoreceptor, vol 1, MIT Press, chap 16, pp 215–233

Chichilnisky EJ, Rieke F (2005) Detection sensitivity and temporal resolution of visual signals near absolute threshold in the salamander retina. J Neurosci 25(2):318–330

Colas F, Droulez J, Wexler M, Bessière P (2007) A unified probabilistic model of the perception of three-dimensional structure from optic flow. Biological Cybernetics 97(5):461–477

Deneve S (2008) Bayesian spiking neurons: inference. Neural computation 20(1):91–117

Dizhoor AM, Hurley JB (1999) Regulation of photoreceptor membrane guanylyl cyclases by guanylyl cyclase activator proteins. Methods (San Diego, Calif) 19(4):521–531

Doya K, Ishii S, Pouget A, Rao RPN (eds) (2007) Bayesian Brain: Probabilistic Approaches to Neural Coding, 1st edn. The MIT Press

Ernst MO, Banks MS (2002) Humans integrate visual and haptic information in a statistically optimal fashion. Nature 415(6870):429–433

Fain GL, Matthews HR, Cornwall MC, Koutalos Y (2001) Adaptation in vertebrate photoreceptors. Physiological reviews 81(1):117–151

Frings S (2009) Primary processes in sensory cells: current advances. Journal of comparative physiology A, Neuroethology, sensory, neural, and behavioral physiology 195(1):1–19

Gold JI, Shadlen MN (2002) Banburismus and the brain: decoding the relationship between sensory stimuli, decisions, and reward. Neuron 36(2):299–308

Hamer RD, Nicholas SC, Tranchina D, Lamb TD, Jarvinen JL (2005) Toward a unified model of vertebrate rod phototransduction. Visual neuroscience 22(4):417–436

van Hateren H (2005) A cellular and molecular model of response kinetics and adaptation in primate cones and horizontal cells. Journal of vision 5(4):331–347

Hodgkin AL, Nunn BJ (1988) Control of light-sensitive current in salamander rods. The Journal of physiology 403:439–471

Jaynes ET (2003) Probability Theory: The Logic of Science. Cambridge University Press

Knill DC, Richards W (eds) (2008) Perception as Bayesian Inference, 1st edn. Cambridge University Press

Koch KW, Stryer L (1988) Highly cooperative feedback control of retinal rod guanylate cyclase by calcium ions. Nature 334(6177):64–66

Körding KP, Wolpert DM (2004) Bayesian integration in sensorimotor learning. Nature 427(6971):244–247

Koutalos Y, Nakatani K, Yau KW (1995) The cgmp-phosphodiesterase and its contribution to sensitivity regulation in retinal rods. The Journal of general physiology 106(5):891–921

Laurens J, Droulez J (2007) Bayesian processing of vestibular information. Biological Cybernetics 96(4):389–404

Ma WJJ, Beck JM, Latham PE, Pouget A (2006) Bayesian inference with probabilistic population codes. Nature neuroscience 9(11):1432–1438

Marr D (1982) Vision: A Computational Investigation into the Human Representation and Processing of Visual Information. The MIT Press

Nikonov S, Lamb TD, Pugh EN (2000) The role of steady phosphodiesterase activity in the kinetics and sensitivity of the light-adapted salamander rod photoresponse. The Journal of general physiology 116(6):795–824

Perlman I, Normann R (1998) Light adaptation and sensitivity controlling mechanisms in vertebrate photoreceptors. Progress in Retinal and Eye Research 17(4):523–563

Pugh EN, Lamb TD (1993) Amplification and kinetics of the activation steps in phototransduction. Biochimica et biophysica acta 1141(2-3):111–149

Pugh EN, Duda T, Sitaramayya A, Sharma RK (1997) Photoreceptor guanylate cyclases: a review. Bioscience reports 17(5):429–473

Pugh EN, Nikonov S, Lamb TD (1999) Molecular mechanisms of vertebrate photoreceptor light adaptation. Current opinion in neurobiology 9(4):410–418

Rabiner LR (1989) A tutorial on hidden markov models and selected applications in speech recognition. Proceedings of the IEEE 77(2):257–286

Rao RPN, Olshausen B, Lewicki MS (eds) (2002) Probabilistic Models of the Brain: Perception and Neural Function, illustrated edition edn. The MIT Press

Rieke F, Baylor DA (1996) Molecular origin of continuous dark noise in rod photoreceptors. Biophysical Journal 71(5):2553–2572

Rieke F, Baylor DA (1998a) Origin of reproducibility in the responses of retinal rods to single photons. Biophysical Journal 75(4):1836–1857

Rieke F, Baylor DA (1998b) Single-photon detection by rod cells of the retina. Reviews of Modern Physics 70(3):1027–1036

Sagoo MS, Lagnado L (1997) G-protein deactivation is rate-limiting for shut-off of the phototransduction cascade. Nature 389(6649):392–395

Shepherd GM (1991) Sensory transduction: entering the mainstream of membrane signaling. Cell 67(5):845–851

Sterling S (2004) How retinal circuits optimize the transfer of visual information, vol 1, MIT Press, chap 17, pp 234–259

Torre V, Ashmore JF, Lamb TD, Menini A (1995) Transduction and adaptation in sensory receptor cells. The Journal of neuroscience : the official journal of the Society for Neuroscience 15(12):7757–7768

Weiss Y, Simoncelli EP, Adelson EH (2002) Motion illusions as optimal percepts. Nature neuroscience 5(6):598–604

Whitlock GG, Lamb TD (1999) Variability in the time course of single photon responses from toad rods: Termination of rhodopsins activity. Neuron 23(2):337–351

Yang T, Shadlen MN (2007) Probabilistic reasoning by neurons. Nature 447(7148):1075–1080

Zemel RS, Dayan P, Pouget A (1998) Probabilistic interpretation of population codes. Neural computation 10(2):403–430